J. Geomag. Geoelectr., **45**, 1001–1012, 1993

Approximate Inverse Mapping Inversion of the COPROD2 Data

Robert G. ELLIS, Colin G. FARQUHARSON, and Douglas W. OLDENBURG

UBC - Geophysical Inversion Facility
Department of Geophysics and Astronomy, University of British Columbia, Vancouver V6T 1Z4, Canada

(Received February 26, 1993; Revised July 29, 1993; Accepted September 3, 1993)

The results of the inversion of the COPROD2 magnetotelluric data set are presented using two implementations of the AIM inverse method. The two algorithms invert magnetotelluric data over 2D conductivity structures. Both algorithms use an approximate inverse mapping based on approximate sensitivities that arise from the 1D conductivity profile beneath each station; this avoids the large computations normally required to approximate the exact inverse mapping, for example, by using the full 2D Jacobian. The primary difference between the algorithms is that the first algorithm minimizes the l_1 norm of the data misfit with regularization provided by minimizing the l_1 norm of the conductivity. This problem is solved with standard linear programming techniques. The second algorithm uses the l_2 norm in place of the l_1 norm and is solved using a subspace approach. Both algorithms produce models with predicted data in satisfactory agreement with the COPROD2 data. The difference between the final models is evidence of the well known nonuniqueness in geophysical inverse problems; the similarities of the final models give a suggestion of that which might be common to all models which fit the data.

1. Introduction

Over the past four years the COPROD2 magnetotelluric (MT) data set (JONES and SAVAGE, 1986; JONES, 1988) has become the de facto standard test for 2D MT inversion programs for several reasons. First, it traverses the North American Central Plains (NACP) anomaly which, being essentially two dimensional, makes it ideal for quantitative analysis via 2D inversion. Second, the data have been "preprocessed" to some extent by the removal of static shift effects, and third, this data set has been inverted by at least two other MT inversion algorithms: Occam (DEGROOT-HEDLIN and CONSTABLE, 1990) and RRI (SMITH and BOOKER, 1991). Consequently, inversion of the COPROD2 data set using the Approximate Inverse Mapping (AIM) technique (OLDENBURG and ELLIS, 1991) will be doubly beneficial: not only might more geophysical constraints be placed on the intriguing NACP anomaly, but a comparison of inversion algorithms will also be possible.

In this paper, we present the results of the inversion of the COPROD2 MT data using two implementations of the AIM inverse method. Both algorithms use an approximate inverse mapping based on approximate sensitivities generated from the 1D conductivity profile beneath each station. This avoids the large computations normally required to approximate the exact inverse mapping, for example, by using the full 2D Jacobian matrix. Here we give only a brief overview of the AIM method per se, and refer the interested reader to OLDENBURG and ELLIS (1991). The primary difference between the two implementations is that the first algorithm minimizes the l_1 norm of the data misfit with regularization provided by minimizing the l_1 norm of the conductivity. This is solved by linear programming techniques. The second algorithm uses the l_2 norm in place of the l_1 norm and is solved using the subspace approach. Here also we will present only a brief overview of the subspace approach and refer the reader to the literature (KENNETT and WILLIAMSON, 1988; OLDENBURG and ELLIS, 1993). We show that both

algorithms produce models with predicted data in satisfactory agreement with the COPROD2 data.

It is well known that geophysical inverse problems are ill-posed. In particular, there are usually infinitely many models that give rise to predicted data, which, when compared to the observed data, provide satisfactory agreement. Consequently, the result of any single inversion cannot be relied upon to represent the true earth. It is necessary to explore the *class* of models which "fit the data" before any meaningful conclusion can be reached. In this vein, the l_1 and l_2 AIM implementations produce significantly different models. The difference between the final models is evidence of nonuniqueness; the similarities of the final models gives a suggestion of the features that might be common to all the models which "fit the data" and hence which might represent the true Earth.

2. Inversion Algorithms

Great flexibility exists in setting up any inverse problem. We begin by presenting details about our choices for: (1) forward modelling, (2) data, (3) model parameterization and (4) sensitivities. These items are the same for both algorithms. Explicit details about the model norm to be minimized and the method of solution will be given after these four items have been considered.

(1) For the forward mapping, the 2D conductivity model is first divided up into rectangular elements. The model is partitioned into n_y horizontal cells and n_z vertical cells and the 2D conductivity $\sigma(y,z)$ is partitioned into an $n_z \times n_y$ array $\sigma_{ij}, i = 1,\ldots,n_z; j = 1,\ldots,n_y$. The thickness of the cells increases (usually logarithmically) with depth. Lateral partitioning in the survey region is dictated by the observation locations which are specified to be at the center of each surface cell. This grid is terminated laterally by uniform layers and below by prisms elongated with depth. The conductivity is assumed to be constant in each cell and the $2D$ MT responses are computed using a transmission surface modelling code (MADDEN, 1972).

(2) TE or TM impedances at n_y observation sites and at n_f frequencies can be inverted individually, jointly, or as determinant averages. Determinant average impedances are generated by

$$Z_{det} = (Z_{xx}Z_{yy} - Z_{xy}Z_{yx})^{1/2} \tag{1}$$

(BERDICHEVSKY and DIMITRIEV, 1976, p. 208). When data are provided in the form of apparent resistivity and phase we transform these to the response

$$R_{jl} = \mu_0 \frac{H(y_j,0,\omega_l)}{E(y_j,0,\omega_l)} \qquad j = 1,\ldots,n_y;\ l = 1,\ldots,n_f \tag{2}$$

where E and H are the electric and magnetic field strengths measured at the j^{th} station located at y_j and with angular frequency ω_l. We choose as data the amplitude and phase of R_{jl}. Errors in the observations are converted by numerical simulation assuming that these errors are Gaussian, unbiased and independent.

(3) For the 2D MT inverse problem we choose $\ln(\sigma)$ as the "model". We let $m_{ij}, i = 1,\ldots,n_z; j = 1,\ldots,n_y$ denote the cellularized array of $\ln(\sigma_{ij})$ values. This cellular parameterization is the same as that used for the forward modelling.

(4) Following OLDENBURG and ELLIS (1991), we begin by defining the exact forward mapping $\mathcal{F}$ to be that which maps the conductivity model into the data response,

$$\mathcal{F} : m(y,z) \longrightarrow R(y;\omega). \tag{3}$$

Linearizing, in the z direction, about a model $m^{(n)}$ yields

$$\mathcal{F}[m;\omega]|_{y=y_0} = \mathcal{F}[m^{(n)};\omega]|_{y=y_0} + \int_0^\infty g_{1D}[m^{(n)};y_0,z,\omega](m(y_0,z) - m^{(n)}(y_0,z))dz + \ldots \quad (4)$$

where g_{1D} is the $1D$ kernel function associated with the conductivity $\sigma(y,z)$ at model offset $y = y_0$ and the superscript denotes the n^{th} iteration. The form of g_{1D} for the amplitude and phase responses used here is given by, OLDENBURG (1979, Eq. 7)

$$g_{1D}[m^{(n)};y_0,z,\omega] = \mu_0\sigma^{(n)}(y_0,z)\left(\frac{E(y_0,z,\omega)}{E(y_0,0,\omega)}\right)^2 \quad (5)$$

where $E(y_0,z,\omega)$ is the electric field strength at the point (y_0,z). In the simplest approximation $E(y_0,z,\omega)$ is taken to be the E field in a 1D earth with conductivity $\sigma(y_0,z)$. This assumes that the E field in the 2D conductivity structure differs only slightly from that in a purely 1D model with conductivity $\sigma(z) = \sigma(y_0,z)$. The positive attributes and limitations of using these sensitivities are illustrated in OLDENBURG and ELLIS (1993). A better approximation to the sensitivities is that of SMITH and BOOKER (1991) in which it is recognized that the E field may show a significantly different z-dependence from the field in the 1D model given by $\sigma(y_0,z)$. But these improved sensitivities now assume that the horizontal derivatives of the E field in the 2D model conductivity structure are small. This second form of the approximate sensitivities is also given by Eq. (5) but with the E field calculated from the 2D model conductivity structure. It should be noted that the first form of the approximate sensitivities based on the E field in the 1D model is the same for both the TE and TM modes.

3. AIM-DS l_1 Norm Inversion Algorithm

The basic AIM-DS equation (OLDENBURG and ELLIS, 1991) is

$$\tilde{\mathcal{F}}[m^{(n+1)}] = d^{obs} + \tilde{\mathcal{F}}[m^{(n)}] - \mathcal{F}[m^{(n)}], \quad (6)$$

where $\mathcal{F}$ denotes a true forward mapping, $\tilde{\mathcal{F}}$ denotes an approximate forward mapping, and d^{obs} denotes the data to be inverted. Defining the approximate forward mapping by keeping only the first two terms in Eq. (4) yields

$$\tilde{\mathcal{F}}[m;\omega]|_{y=y_0} = \mathcal{F}[m^{(n)};\omega]|_{y=y_0} + \int g_{1D}[m^{(n)};y_0,z,\omega](m(y_0,z) - m^{(n)}(y_0,z))dz, \quad (7)$$

and substituting into Eq. (6) yields

$$\int g_{1D}[m^{(n)};y_0,z,\omega]m^{(n+1)}(z)dz = d^{obs}(y_0,\omega) - d^{(n)}(y_0,\omega) + \int g_{1D}[m^{(n)};y_0,z,\omega]m^{(n)}(z)dz. \quad (8)$$

Discretizing this equation produces

$$\sum_i^{n_z} A_{ijk}m_{ij}^{(n+1)} = d_{jk}^{obs} - d_{jk}^{(n)} + \sum_i^{n_z} A_{ijk}m_{ij}^{(n)} \equiv B_{jk} \qquad j = 1,\ldots,n_y;\ k = 1,\ldots,2n_f \quad (9)$$

where A_{ijk} is the integral of the k^{th} $1D$ kernel function g_{1D} at model offset y_j over the i^{th} depth partition.

At this stage the inverse problem has been reduced to the solution of a set of simultaneous equations. Under usual circumstances the matrix A is poorly conditioned and must be regularized before a meaningful solution is obtained. A measure of the misfit between the predicted data and the observed data can be defined by ϕ_d,

$$\phi_d = \sum_j^{n_y} \sum_k^{2n_f} \left| \sum_i^{n_z} \frac{A_{ijk} m_{ij}^{(n+1)} - B_{jk}}{\epsilon_{jk}} \right| \tag{10}$$

where ϵ_{jk} is the standard deviation of the datum R_{jk}^{obs}. Regularization of the inverse problem can be achieved by defining a model norm objective function,

$$\begin{aligned} \phi_m &= \beta \int \left| \frac{dm}{dy} \right| dydz + \gamma \int \left| \frac{dm}{dz} \right| dydz \\ &= \beta \sum_i^{n_z} \sum_j^{n_y - 1} \Delta z_i |m_{i,j+1}^{(n+1)} - m_{i,j}^{(n+1)}| + \gamma \sum_i^{n_z - 1} \sum_j^{n_y} \Delta y_j |m_{i+1,j}^{(n+1)} - m_{i,j}^{(n+1)}|. \end{aligned} \tag{11}$$

The inverse problem is solved by minimizing the objective function,

$$\phi = \phi_m + \mu \phi_d. \tag{12}$$

The parameters β and γ control the relative weighting of the x and z variations and are fixed for each inversion. The Lagrange multiplier μ is generally sought by trial and error so that the final misfit achieves a target value consistent with the errors associated with the data. However, rather than start with this final value of μ, a schedule of μ values is found to be desirable. This schedule is a monotonically increasing sequence which asymptotes to a constant. The increasing nature of μ prevents unnecessary roughness being accumulated in the model at intermediate steps. Although this approach has the possible disadvantage that a non-optimum sequence of μ's may be selected, the major advantage is that only one forward modelling need be carried out per iteration. This may be compared to the approach where a schedule of target misfits is chosen and then a line search performed to find the corresponding Lagrange multiplier μ at each iteration. Of course, with this second approach there is the possible disadvantage that a non-optimum sequence of target misfits may be selected with the associated non-optimum number of line searches. Although the best approach is somewhat model dependent, we find, in general, that the computational savings associated with a simple schedule of μ values can be substantial because line searches typically involve 3 to 8 forward modellings.

The use of the l_1 norm requires the definition of an appropriate misfit measure. Here we follow PARKER and MCNUTT (1980) and define

$$\chi_N^1 = \frac{1}{2n_f n_y} \sqrt{\frac{\pi}{2}} \sum_k^{2n_f} \sum_j^{n_y} \left| \frac{R_{jk}^{obs} - R_{jk}^{(n)}}{\epsilon_{jk}} \right|. \tag{13}$$

Note that $E[\chi_N^1] = 1$.

The problem of minimizing (12) is solved using linear programming (LP) techniques. Here, we simply note that minimization of an l_1 model norm gives rise to models with large regions of constant conductivity, i.e., block type models, and the use of an l_1 data norm provides robustness in the presence of noise on the data. These two characteristics of the l_1 norm are well suited to inverting MT data with static shift effects.

4. AIM-MS l_2 Norm Inversion Algorithm

The blockiness of models produced by the l_1 norm inversion may be a desirable characteristic for some earth geologies, but other geological environments might be better emulated by smoother models. Correspondingly, we present an algorithm that minimizes the l_2 norm of the conductivity model. In this algorithm, we incorporate a reference model in the objective function so that structure is minimized with respect to this reference model.

In the l_1 norm inversion the model is found by explicitly solving for the conductivity in each cell. Effectively, each cell is a basis element in model space and finding values of the conductivities requires solving a large matrix system. This is quite efficient for the sparse LP solver XMP (MARSTEN, 1981) given the size of problem considered in this paper. The l_2 norm inversion however requires the solution of an $M \times M$ system of equations where M is the number of cells in the model. This computation can become prohibitive as the number of cells increases. To obviate this difficulty, we appeal to a generalized subspace methodology. We adopt the formalism outlined in OLDENBURG *et al.* (1993) but present only the essence of the calculation here.

The basic AIM-MS equation is

$$m^{(n+1)} = m^{(n)} + \tilde{\mathcal{F}}^{-1}[d^{obs}] - \tilde{\mathcal{F}}^{-1}\mathcal{F}[m^{(n)}] \tag{14}$$

where $\tilde{\mathcal{F}}^{-1}$ denotes an approximate inverse mapping defined such that $\tilde{\mathcal{F}}\tilde{\mathcal{F}}^{-1} = \mathcal{I}_e$ where $\mathcal{I}_e$ is the identity operator in data space. Equation (14) can be rewritten:

$$\delta m^{(n)} \equiv m^{(n+1)} - m^{(n)} = \tilde{\mathcal{F}}^{-1}[d^{obs}] - \tilde{\mathcal{F}}^{-1}[d^{(n)}]. \tag{15}$$

After discretizing, Eq. (15) becomes schematically

$$\delta m_{ij}^{(n)} = A_{ijk}^{-1} d_{jk}^{obs} - A_{ijk}^{-1} d_{jk}^{(n)} \qquad i = 1, \ldots, n_z \tag{16}$$

where A_{ijk} is the integral of the k^{th} $1D$ kernel function g_{1D} at model offset y_j over the i^{th} depth partition and A^{-1} is the inverse of the matrix A.

As before, the inverse problem has been reduced to the solution of a set of simultaneous equations involving a poorly conditioned matrix A. We proceed in the usual manner by defining a data misfit objective function, ϕ_d, and a model norm objective function, ϕ_m. We define the data misfit objective function,

$$\phi_d = \sum_{j}^{n_y} \sum_{k}^{2n_f} \left(\frac{d_{jk}^{obs} - d_{jk}}{\epsilon_{jk}} \right)^2 . \tag{17}$$

Assuming the measurement errors ϵ_{jk} arise from Gaussian random noise, the expected value for ϕ_d is $2n_f n_y$.

Our choice for the model norm ϕ_m is guided by a desire to find a model which has minimum energy in the vertical and horizontal directions and at the same time is close to a reference model m_0. To accomplish this we minimize a discrete approximation to

$$\phi_m = \iint \left\{ \alpha_s w_s (m - m_0)^2 + \alpha_y w_y \left(\frac{\partial (m - m_0)}{\partial y} \right)^2 + \alpha_z w_z \left(\frac{\partial (m - m_0)}{\partial z} \right)^2 \right\} dy dz. \tag{18}$$

The parameters α_s, α_y and α_z, which are fixed for each inversion, control the relative weighting of the smallest model component and the y and z variations. The weighting functions $w_s(y, z)$,

$w_y(y,z)$ and $w_z(y,z)$ provide additional flexibility to control the characteristics of the final model. The model norm used in the inversion is therefore

$$\phi_m = \|\mathbf{W_m}(\mathbf{m} - \mathbf{m_0})\|^2 \tag{19}$$

where the weighting matrix $\mathbf{W_m}$ is determined from α_s, α_y and α_z, and from $w_s(y,z)$, $w_y(y,z)$ and $w_z(y,z)$.

The total objective function to be minimized is then

$$\phi = \phi_m + \mu(\phi_d - \phi_d^*) \tag{20}$$

where μ is again a Lagrange multiplier and ϕ_d^* is some target misfit consistent with the errors associated with the observations. A schedule of the target ϕ_d^* values at each iteration is found to be desirable. This schedule is a monotonically decreasing sequence which asymptotes to the desired misfit. The process prevents unnecessary roughness being accumulated in the model at early and intermediate steps. A line search is required at each iteration to find the Lagrange multiplier μ corresponding to the value of ϕ_d^* sought at that particular iteration.

In a subspace approach to the solution of Eq. (20), the model perturbation $\delta\mathbf{m}$ is restricted to lie in a q-dimensional subspace ($q << M$) which is spanned by the vectors $\{\mathbf{v}^r : r = 1, q\}$. The model perturbation can be written as

$$\delta\mathbf{m} = \sum_{r=1}^{q} \alpha^r \mathbf{v}^r = \mathbf{V}\alpha \tag{21}$$

and is therefore specified once the parameters α^r are determined.

The subspace equations are generated by substituting (21) into (20) and differentiating with respect to α^r:

$$\mathbf{V^T}(\mathbf{W_m^T W_m} + \mu\mathbf{A^T A})\mathbf{V}\alpha = -\mu\mathbf{V^T A^T}\delta\mathbf{d} - \mathbf{V^T W_m^T W_m}(\mathbf{m} - \mathbf{m_0}). \tag{22}$$

At each iteration a line search over possible values of μ is performed to find the value of μ so that, after Eq. (22) is solved for α, the corresponding model gives rise to a value of ϕ_d equal to the value of ϕ_d^* required for that iteration. Convergence is reached when the data misfit is satisfactory and the model norm is minimized.

The success of the subspace methodology depends strongly upon the choice of basis vectors. In OLDENBURG *et al.* (1993) considerable success was achieved by subdividing the misfit objective function and using steepest descent vectors associated with each subdivision of the data. Here we segment the data misfit objective function according to frequency, amplitude and phase. The r^{th} search vector becomes

$$\mathbf{v^r} = (\mathbf{W_m^T W_m})^{-1}\nabla_\mathbf{m} \sum_{j=1}^{n_y} \left(\frac{R_{jr}^{obs} - R_{jr}^{(n)}}{\epsilon_{jr}} \right)^2 \qquad r = 1, \ldots, 2n_f \tag{23}$$

where each datum in the summation is an amplitude (or phase) at a single frequency, and $\nabla_\mathbf{m}$ represents the gradient with respect to the model $\mathbf{m}$. Every inversion carried out contains these vectors, as well as the constant vector and $(\mathbf{W_m^T W_m})^{-1}\nabla_\mathbf{m}\phi_m = \mathbf{m^{(n)}} - \mathbf{m_0}$, which is the steepest descent vector associated with the model objective function. In addition, we also segment the model norm objective function and form steepest descent vectors from each of these minor objective functions. The segmentation is invoked by choosing a rectangular region of the model and subdividing this region into smaller groups. The projection of $(\mathbf{m^{(n)}} - \mathbf{m_0})$ onto any group of

cells provides a new search direction. The rectangular region can be the entire model or a smaller portion of particular interest. In the initial iterations we have used each row of cells to make a basis vector, and have also subdivided the entire model into groupings of $n \times n$ cells where n is typically 5. At later iterations, when features of interest have appeared, we have centered the rectangle over these features to see if structure is enhanced or attenuated in a subsequent iteration. This process can be both interactive and dynamic. The attractive aspect of the dynamic use of additional search vectors is that in the subspace inversion only a model perturbation is sought. At worst, a poor choice of vectors produces little benefit.

5. COPROD2 Data Set l_1 Norm Inversion

We now invert a subset of the COPROD2 data set provided by A. G. Jones. These data were collected along an east-west traverse in Southern Saskatchewan and Manitoba in Canada. There are 35 stations with spacings of approximately 10 km. The data have been analysed by JONES and SAVAGE (1986) and JONES (1988) and have been distributed as test data for 2D inversion algorithms. We now present the results of the application of the AIM l_1 inversion to a subset of the COPROD2 data. The subset chosen consists of the data at all 35 stations and at the 8 periods: 5.3, 10.7, 21.3, 42.9, 85.5, 170.6, 341.3, and 684.9 seconds. From this subset we have extracted both the TE mode and TM mode data to form a joint data set. Following DEGROOT-HEDLIN and CONSTABLE (1990) we attribute minimum errors of $\pm 10\%$ to the apparent resistivities and ± 5 degrees to the phases.

In order to generate a starting model for the inversion the COPROD2 data were converted to determinant data, Eq. (1) and inverted (OLDENBURG and ELLIS, 1993) using 1D sensitivities, Eq. (5) with the $E(y_0, z)$ field derived from a one dimensional earth under each site. This produced the starting model shown in Fig. 1a and the fit to the observed determinant average data shown on Fig. 2a.

A first attempt was made to jointly invert the TE and TM mode COPROD2 data using an approximate inverse mapping based on 1D sensitivities, Eq. (5) with the $E(y_0, z)$ field derived from a one dimensional earth under each site. However a satisfactory inversion result could only be achieved when the approximate inverse mapping was based on the 1D sensitivities, Eq. (5) with the 2D $E(y_0, z)$ field derived from a two dimensional earth under each site. Using the 1D E fields resulted in extremely poor convergence. The result of the successful inversion of the joint TE and TM mode data ($\beta : \gamma = 1 : 1$) is shown in Fig. 1b and the observed and predicted data are shown in Fig. 2b. The predicted data have a normalized misfit $\chi^1_N = 1.15$. We were unable to reduce the misfit to $\chi^1_N = 1$ without increasing the number of cells in the model. Even at the $\chi^1_N = 1.15$ misfit level, the NACP anomaly is clearly resolved into three conductors at a depth of 20 km and dipping to the west. The TOBE anomaly is clearly resolved as a strong conductor at 10 km depth. These results confirm, in a general sense, the finding of other workers (DEGROOT-HEDLIN and CONSTABLE, 1990) who have inverted this data set.

6. COPROD2 Data Set l_2 Norm Inversion

The AIM l_2 norm inversion described in Section 4 was then used to invert the same subset of the COPROD2 data set described in Section 5 above. The result of inverting the determinant averaged data with the l_2 norm inversion is shown in Fig. 1c. This model gave predicted data shown in Fig. 3a and was used as the starting model for the l_2 norm joint inversion.

As with the l_1 norm inversion, an attempt was made to invert the joint TE and TM mode data set using the 1D approximate sensitivities defined in Eq. (5). Using these sensitivities, the algorithm did a poor job of reproducing the significant differences between the TE and TM mode responses that can be seen in the COPROD2 data. This failure is not surprising since the 1D

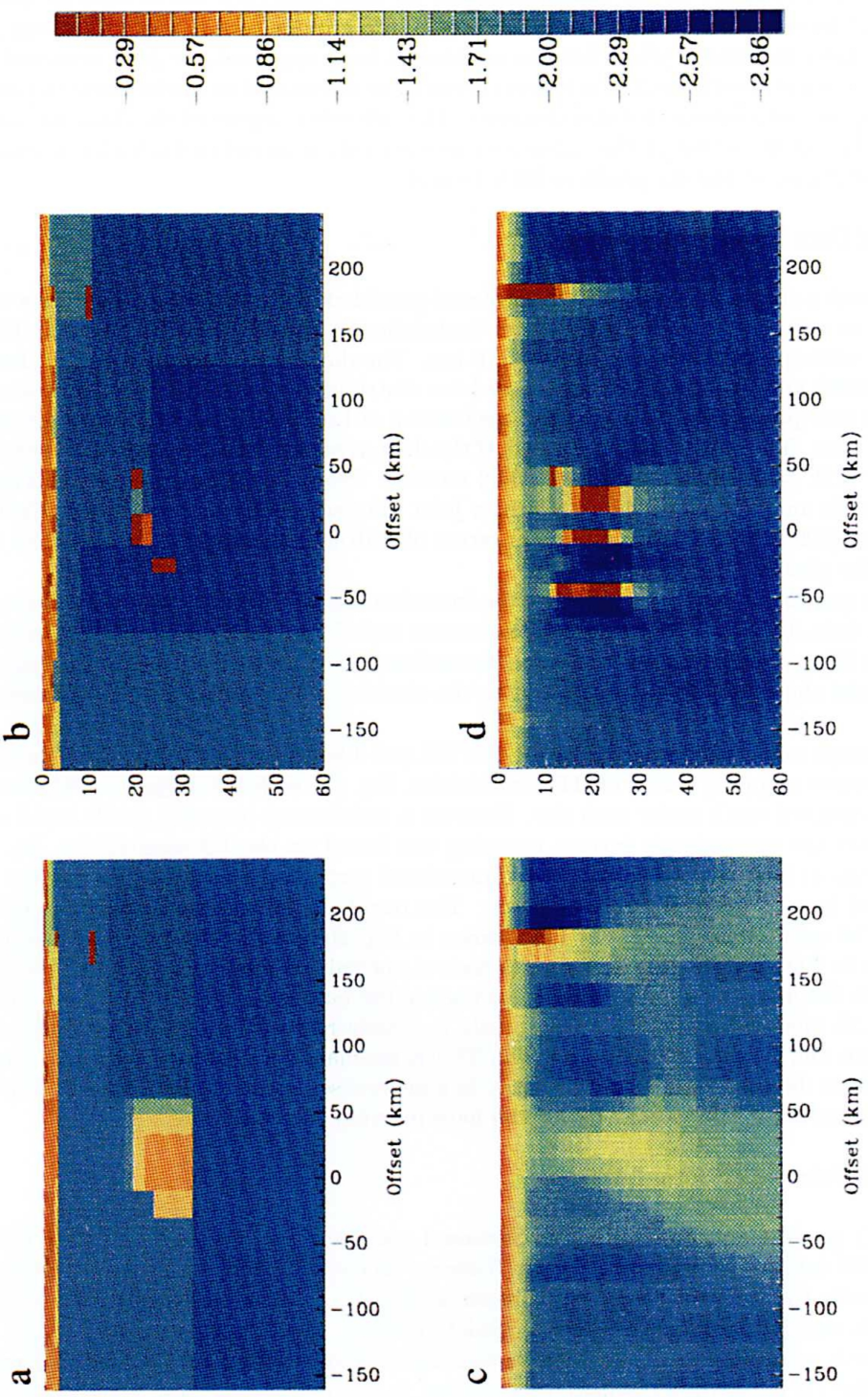

Fig. 1. Panels (a) and (b) are the models obtained from the l_1 inversion of the COPROD2 (a) determinant data and (b) joint TE and TM mode data. Panels (c) and (d) are the models obtained from the l_2 inversion of the COPROD2 (c) determinant data and (d) joint TE and TM mode data. The colour bar shows the $\log_{10}$ conductivity.

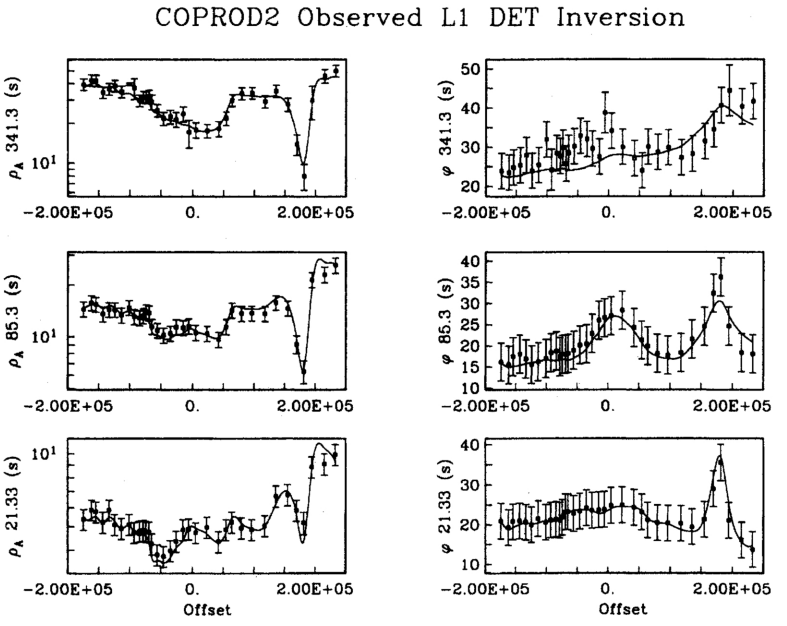

(a)

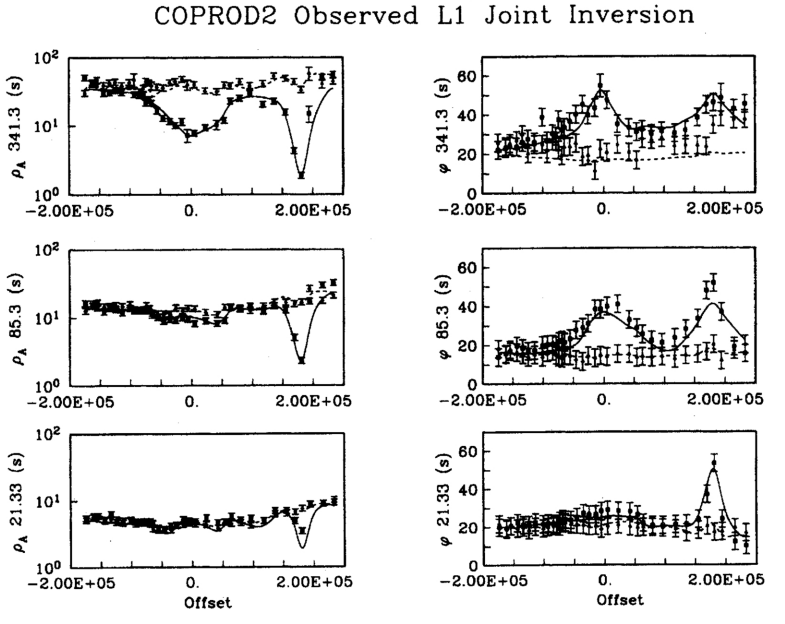

(b)

Fig. 2. Panels (a) and (b) are the observed data (points with error bars) and the predicted data (curves) obtained with the models produced by the l_1 inversion of the COPROD2 (a) determinant data and (b) joint TE (solid) and TM (dashed) mode data.

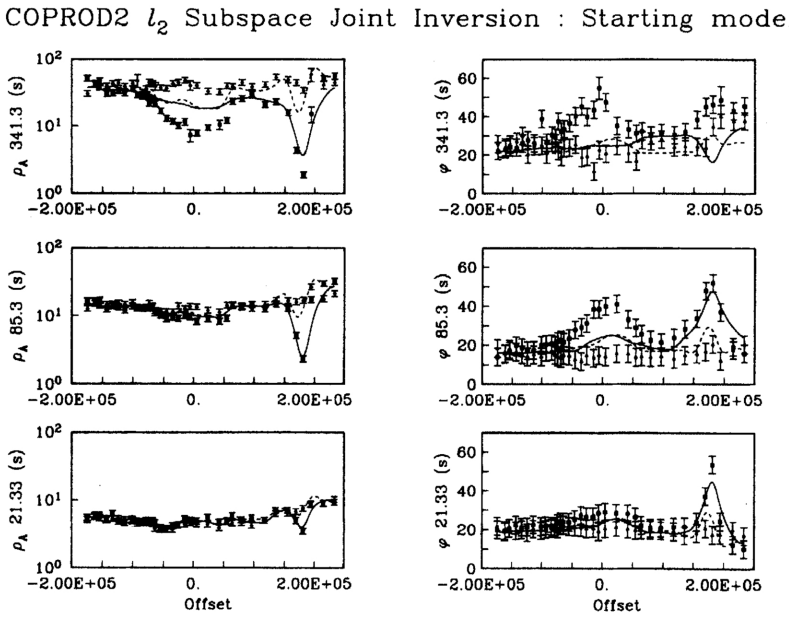

(a)

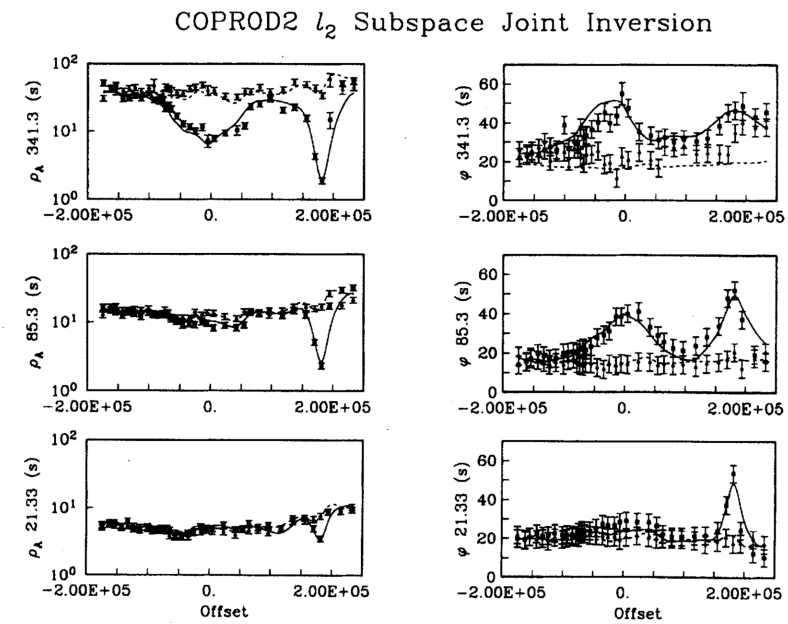

(b)

Fig. 3. Panels (a) and (b) are the observed data (points with error bars) and the predicted data (curves) obtained with the models produced by the l_2 inversion of the COPROD2 (a) determinant data and (b) joint TE (solid) and TM (dashed) mode data.

approximate sensitivities in Eq. (5), which use the $E(y_0, z)$ field calculated for a 1D earth below each site, are identical for both the TE and TM modes, whereas the COPROD2 TE and TM data have very different structure.

The COPROD2 joint TE and TM mode data set was then inverted using the modified sensitivities described at the end of Section 2 which make use of the E and H fields calculated from the 2D conductivity structure. The resulting model is shown in Fig. 1d and the predicted data in Fig. 3b. The value of the normalized χ^2 misfit for this model was $\chi^2_N = 2.5$. For the initial iterations, the model was divided up into large-scale features, such as rows, columns or 5×5 blocks of cells. These provided additional basis vectors onto which $(\mathbf{m^{(n)}} - \mathbf{m_0})$ could be projected to produce new search directions. Later in the inversion process, once features associated with the NACP and TOBE anomalies began to appear, smaller groupings of cells (e.g., 2×2, 3×1, 1×1) were used over the extent of these features in order to improve resolution.

The value of misfit for the model shown in Fig. 1d, $\chi^2_N = 2.5$, is not as low as the expected value, $E[\chi^2_N] = 1$, given the stated errors on the observations. However, this did appear to be the limit of this algorithm when based on these approximate sensitivities, and on the coarse horizontal discretisation forced upon the algorithm by only having sensitivities defined for cells directly below observation locations. However, as can be seen from Fig. 3b, the model in Fig. 1d does produce predicted data which have a qualitative resemblance to the observations. And, once again, the conductor associated with the TOBE anomaly and the three conductors associated with the NACP anomaly are clearly visible in the model.

7. Discussion

The MT inverse problem associated with inverting the COPROD2 data is ill-posed. This makes it difficult to invert the COPROD2 data to produce meaningful information about the Earth's conductivity structure. Unfortunately, the inversion process involves a sequence of "educated guesses" to enable a *single* model to be constructed. The main "educated guess" concerns what form of the model objective function is to be minimized. To gain meaningful information from the inversion of the COPROD2 data, the effect of the "educated guesses" must be ascertained. Consequently, the COPROD2 data set must be inverted not once, but many times with different guesses, and practicality demands that the inversion computation be efficient. We have shown that working with AIMs and determinant average data, at least in the formative stages of the inversion, keeps the inverse problem smaller and avoids the difficulties associated with inaccurate phase rotations of the impedance tensor and perhaps other processing difficulties. Our l_1 and l_2 inversion results from the determinant average data provide a definite indication of the NACP and TOBE conductivity anomalies and provide end members in the spectrum of possible conductivity models: the l_1 result is the most blocky model; the l_2 result is the most smooth. The l_1 and l_2 inversions demonstrate that very different models can be produced by altering the objective function to be minimized. This exploration provides a greater understanding about the resolving power of the COPROD2 data.

Numerical efficiency in both the l_1 and l_2 algorithms was achieved through the use of 1D sensitivities. These sensitivities are surprisingly beneficial in 2D problems, at least if misfits of about 10 percent on the apparent resistivities and 5 degrees on the phase are adequate. The fact that the 1D sensitivities work as well as they do suggests that rather crude approximations to $2D$ sensitivities may work extremely well within the AIM technique. However for the successful joint inversion of the COPROD2 data, which have very different TE and TM mode responses, it was necessary to modify the purely 1D approximation to include the 2D field variation. The results obtained from this improved approximation motivates further research into developing even better approximations which are still computationally less demanding than carrying out an accurate 2D linearization.

In conclusion, we emphasize that the fundamental difficulty with the COPROD2 MT inverse problem is that it is ill-posed. Of particular concern is the inherent nonuniqueness which can only be addressed by considering the class of models which fit the COPROD2 data to the desired level. One method for exploring the class of models is by performing a significant number of inversions with different model norms, and this can only be done if inversion algorithms are flexible and efficient. The AIM algorithms presented in this paper were designed with flexibility and efficiency as a highest priority and we have shown that they provide the means for a preliminary investigation of the COPROD2 data.

The authors wish to thank A. G. Jones for supplying the COPROD2 data and P. Savage of Pan-Canadian for making the data available to the GSC. The authors are also grateful to the University of Waterloo, Department of Computer Science for making available the MAT1 sparse matrix solver (D'AZEVEDO, 1991). The authors thank S. Constable and an anonymous referee for comments which improved the final manuscript. CGF gratefully acknowledges receipt of a Commonwealth Scholarship. This work was partially supported by NSERC grant 5-84270.

REFERENCES

BERDICHEVSKY, M. N. and V. I. DIMITRIEV, Basic principles of interpretation of magnetotelluric sounding curves, in *Geoelectric and Geothermal Studies*: *KAPG Geophysical Monograph*, pp. 165–221, Akad, Kiado, 1976.

CONSTABLE, S. C., R. L. PARKER, and C. G. CONSTABLE, Occam's inversion: A practical algorithm for generating smooth models from electromagnetic sounding data, *Geophysics*, **52**, 289–300, 1987.

D'AZEVEDO, E. F. KNIGHTLEY, and P. A. FORSYTH, *MAT1 Iterative Sparse Matrix Solver*: *User's Guide*, Department of Computer Science, University of Waterloo, 1991.

DEGROOT-HEDLIN, C. and S. C. CONSTABLE, Occam's inversion to generate smooth, two-dimensional models from magnetotelluric data, *Geophysics*, **55**, 1613–1624, 1990.

JONES, A. G., Static shift of magnetotelluric data and its removal in a sedimentary basin, *Geophysics*, **53**, 967–978, 1988.

JONES, A. G. and P. J. SAVAGE, North American Central Plains conductivity anomaly goes east, *Geophys. Res. Lett.*, **13**, 685–688, 1986.

KENNETT, B. L. N. and P. R. WILLIAMSON, Subspace methods for large-scale nonlinear inversion, in *Mathematical Geophysics*: *A Survey of Recent Developments in Seismology and Geodynamics*, edited by N. J. Vlaar, G. Nolet, M. J. R. Wortel, and S. A. P. L. Cloetingth, D.Reidel, Dordrecht, 1988.

MADDEN, T. R., Transmission systems and network analogies to geophysical forward and inverse problems, Tech. Rep., Department of Earth and Planetary Sciences, MIT, **72-3**, 1972.

MARSTEN, R. E., The design of the XMP linear programming library, *ACM Trans. Math. Software*, **7**, 481–497, 1981.

OLDENBURG, D. W., One-dimension inversion of natural source magnetotelluric observations, *Geophysics*, **44**, 1218–1244, 1979.

OLDENBURG, D. W. and R. G. ELLIS, Inversion of geophysical data using an approximate inverse mapping, *Geophys. J. Int.*, **105**, 325–353, 1991.

OLDENBURG, D. W. and R. G. ELLIS, Efficient inversion of magnetotelluric in two dimensions, *Phys. Earth Planet. Inter.*, V. R. S. Hutton Symposium, 1993 (in press).

OLDENBURG, D. W., P. R. MCGILLIVRAY, and R. G. ELLIS, Generalized subspace methods for large scale inverse problems, *Geophys. J. Int.*, **114**, 12–20, 1993.

PARKER, R. L. and M. K. MCNUTT, Statistics for the one-norm misfit measure, *J. Geophys. Res.*, **85**, 4429–4430, 1980.

SMITH, J. T. and J. R. BOOKER, Rapid inversion of two- and three-dimensional magnetotelluric data, *J. Geophys. Res.*, **96**, 3905–3922, 1991.